Computational and Structural Biotechnology Journal 21 (2023) 3760–3767

Contents lists available at ScienceDirect

Computational and Structural Biotechnology Journal

journal homepage: www.elsevier.com/locate/csbj

Research article

Structural basis of the specificity and interaction mechanism of Bmf binding to pro-survival Bcl-2 family proteins

Haolan Wang [a], Ming Guo [a], Hudie Wei [a,*], Yongheng Chen [a,b,**,1]

[a] Department of Oncology, NHC Key Laboratory of Cancer Proteomics, Laboratory of Structural Biology, National Clinical Research Center for Geriatric Disorders, Xiangya Hospital, Central South University, Changsha, Hunan 410008, China
[b] National Clinical Research Center for Geriatric Disorders, Xiangya Hospital, Central South University, Changsha, Hunan 410008, China

ARTICLE INFO

Keywords:
Bcl-2 family proteins
Apoptosis
Pro-survival Bcl-2 family protein
BH3-only protein
Bmf

ABSTRACT

The apoptotic pathway is regulated by protein-protein interactions between members of the Bcl-2 family. Pro-survival Bcl-2 family proteins act as cell guardians and protect cells against death. Selective binding and neutralization of BH3-only proteins with pro-survival Bcl-2 family proteins is critical for initiating apoptosis. In this study, the binding assay shows that the BH3 peptide derived from the BH3-only protein Bmf has a high affinity for the pro-survival proteins Bcl-2 and Bcl-xL, but a much lower affinity for Mcl-1. The complex structures of Bmf BH3 with Bcl-2, Bcl-xL and Mcl-1 reveal that the α-helical Bmf BH3 accommodates into the canonical groove of these pro-survival proteins, but the conformational changes and some interactions are different among the three complexes. Bmf BH3 forms conserved hydrophobic and salt bridge interactions with Bcl-2 and Bcl-xL, and also establishes several hydrogen bonds to support their binding. However, the highly conserved Asp-Arg salt bridge is not formed in the Mcl-1/Bmf BH3 complex, and few hydrogen bonds are observed. Furthermore, mutational analysis shows that substitutions of less-conserved residues in the α2-α3 region of these pro-survival Bcl-2 family proteins, as well as the highly conserved Arg, lead to significant changes in their binding affinity to Bmf BH3, while substitutions of less-conserved residues in Bmf BH3 have a more dramatic effect on its affinity to Mcl-1. This study provides structural insight into the specificity and interaction mechanism of Bmf BH3 binding to pro-survival Bcl-2 family proteins, and helps guide the design of BH3 mimics targeting pro-survival Bcl-2 family proteins.

1. Introduction

Bcl-2 family proteins are central regulators of the endogenous apoptotic pathway [1,2]. The delicate balance between pro-survival and pro-apoptotic members determines cell fate. Activation and oligomerization of pro-apoptotic members Bax/Bak in response to cellular stress stimulation leads to mitochondrial outer membrane permeability (MOMP) and initiation of apoptosis [3,4]. Pro-survival proteins, including Bcl-2, Bcl-xL, Bcl-w, Mcl-1 and Bfl-1/A1, inhibit pro-apoptotic proteins and MOMP [5]. Cancer cells frequently overexpress pro-survival Bcl-2 proteins to inhibit apoptotic signaling [6]. BH3-only proteins are a unique group of pro-apoptotic proteins that share only the homologous BH3 domain with other members [5,7,8], and are subdivided into "activators" (Bid, Bim, Puma) and "sensitizers" (Bik, Hrk, Bmf and Noxa) [6]. Activators can isolate pro-survival Bcl-2 family proteins and directly activate Bax/Bak, while sensitizers mainly target pro-survival Bcl-2 family proteins. In either case, the binding of BH3-only proteins to pro-survival Bcl-2 family proteins is required for the activation of pro-apoptotic proteins and subsequent cell death [9–11].

Structural studies have demonstrated a canonical interaction mechanism between BH3-only proteins and pro-survival Bcl-2 family proteins. The BH3 domain of the BH3-only protein, which is characterized by four hydrophobic residues (h1-h4) and an invariant aspartic acid (h3 + 2) (Fig. S1), forms an amphipathic helix and binds to the hydrophobic groove of pro-survival Bcl-2 family proteins. The properties of the BH3

* Corresponding author.
** Corresponding author at: Department of Oncology, NHC Key Laboratory of Cancer Proteomics, Laboratory of Structural Biology, National Clinical Research Center for Geriatric Disorders, Xiangya Hospital, Central South University, Changsha, Hunan 410008, China.
E-mail addresses: hudiewei18@163.com (H. Wei), yonghenc@163.com (Y. Chen).
[1] Lead contact.

https://doi.org/10.1016/j.csbj.2023.07.017
Received 10 April 2023; Received in revised form 18 July 2023; Accepted 19 July 2023
Available online 21 July 2023
2001-0370/© 2023 The Authors. Published by Elsevier B.V. on behalf of Research Network of Computational and Structural Biotechnology. This is an open access article under the CC BY-NC-ND license (http://creativecommons.org/licenses/by-nc-nd/4.0/).

domain as well as the hydrophobic groove result in their binding specificity and selectivity. Given the interaction mechanism, an anti-cancer therapy called "BH3-mimetic drugs" has been developed. These drugs mimic the function of BH3-only proteins, which selectively bind to and antagonize specific pro-survival Bcl-2 family proteins to activate apoptosis in malignant cells [12,13].

Mouse Bmf was first isolated by yeast two-hybrid technique using Mcl-1 as a bait [14]. Under physiological conditions, endogenous Bmf is anchored to the Dynein Light Chain (DYNLL) of the cytoskeleton and constantly senses intracellular changes [15,16]. Once the cell is stimulated by stress, Bmf is transferred to the mitochondria and binds to pro-survival Bcl-2 members to trigger apoptosis [15–17]. Several studies have shown that Bmf and Bim act synergistically [18,19]. Bmf leads to the release of Bim via displacement, while Bim is able to inhibit all pro-survival Bcl-2 family proteins or activate Bak/Bax by binding with high affinity to their canonical BH3 binding groove [20–23]. However, Bmf has been shown to bind and directly activate Bak through an alternative binding groove [24], and Bmf has a strict selectivity toward pro-survival Bcl-2 family proteins [25].

In this study, we determined the binding affinities of Bmf BH3 for the pro-survival proteins Bcl-2, Bcl-xL and Mcl-1, and then resolved the complex structures of Bmf BH3 with Bcl-2, Bcl-xL and Mcl-1. In addition, we analyzed the binding specificity determinant in the sequences of the pro-survival Bcl-2 family proteins and Bmf BH3. These structural and functional analyses elucidate the interaction mechanism of Bmf BH3 selectively binding to pro-survival proteins, and also bring new insights into the development of BH3-mimetic drugs.

2. Results

2.1. Ability of Bmf BH3 binding to Bcl-2, Bcl-xL and Mcl-1

The pro-apoptotic activity of BH3-only protein is mainly manifested by binding ability to pro-survival Bcl-2 family proteins. Hence, we measured the binding affinity of Bmf BH3 toward three pro-survival proteins Bcl-2, Bcl-xL and Mcl-1 by fluorescence polarization assay (FP). We obtained soluble recombinant proteins by removing the C-terminal transmembrane domain of Bcl-2, Bcl-xL and Mcl-1 and the N-terminal PEST region of Mcl-1 (namely Bcl-2ΔC32, Bcl-xLΔC25 and Mcl-1ΔN170ΔC23). A 25-residue fluorescent Bmf peptide (FITC-Bmf BH3) derived from the BH3 domain of Bmf was used. The FITC-Bmf BH3 bound tightly to Bcl-2 and Bcl-xLwith dissociation constant (Kd) values of 5.2 nM and 5.1 nM, respectively, while its binding affinity for Mcl-1 was decreased by 40-fold with a Kd of 185 nM (Table 1). The different binding abilities of Bmf BH3 to Bcl-2, Bcl-xL and Mcl-1 may indicate their functional distinction in the apoptotic process [26,27].

2.2. Conformational changes in the α2-α4 region of Bcl-2, Bcl-xL and Mcl-1 upon binding to Bmf BH3

To further understand the binding specificity of Bmf to different pro-survival Bcl-2 family proteins, we tried to determine their structures by X-ray crystallography. For crystallization, we used Bcl-2 and Bcl-xL constructs with large unstructured loops removed. We used a 25-mer Bmf BH3 peptide and a 21-mer Bmf BH3 peptide to crystallize with these proteins and obtained the structures of Bcl-xL (Bcl-xLΔC25ΔLoop) with 25-mer Bmf BH3 peptide, Bcl-2 (Bcl-2ΔC32ΔLoop) with 21-mer Bmf BH3 peptide and Mcl-1 (Mcl-1ΔN170ΔC23) with 21-mer Bmf BH3 peptide with resolutions of 2.88, 2.96 and 1.96 Å, respectively (Table S1-2). Compared to the apo structures [28–30], Bmf BH3 induces different conformational changes in these pro-survival proteins. In the Bcl-2/Bmf BH3 complex, the α2 terminal and α3 helix of Bcl-2 shift away to accommodate the Bmf BH3 peptide (Fig. 1A). Bcl-xL forms an opened V-shaped structure with α4 close to the peptide and α3 becoming less helical and away from the Bmf BH3 peptide (Fig. 1B). Moreover, the orientation of Tyr-101 and Phe-105 at the α2-α3 junction shifted. This conformational shift is also observed in the structures of Bcl-xL with Bim BH3 (PDB: 4QVF) [31], Bid BH3 (PDB: 4QVE) [31], Bak BH3 (PDB: 1BXL) [32] and Puma BH3 (PDB: 2M04) [33], and the structure of Bcl-2 with Bax BH3 peptide (PDB: 2XA0) [34]. In contrast to the major conformational changes at the α2, α3 and α4 regions of Bcl-2 and Bcl-xL, Mcl-1 conformation in the Mcl-1/Bmf BH3 structure is slightly changed from the apo structure upon binding to Bmf (Fig. 1C).

Although the overall structures of Bmf BH3 in complex with Bcl-2, Bcl-xL and Mcl-1 have high similarity, each structure displays unique features. To better understand specificity determinants of pro-survival Bcl-2 family proteins and BH3, we then made a detailed comparison of hydrophobic and hydrophilic interactions in these complexes.

Table 1
Binding affinities of Bim BH3 and Bmf BH3 with Bcl-2, Bcl-xL and Mcl-1.

Proteins / Peptide (Kd)	Bcl-2	Bcl-xL	Mcl-1
Bim BH3	6.1 ± 0.3 nM	4.4 ± 0.9 nM	5.8 ± 0.1 nM
Bmf BH3	5.2 ± 0.3 nM	5.1 ± 0.4 nM	185 ± 9.6 nM

Fluorescence polarization assay was performed to determine the dissociation constants (Kd) of fluorescently labeled Bim BH3 or Bmf BH3 bound to Bcl-2, Bcl-xL, and Mcl-1. All assays were independently performed three times, and Kd was determined by nonlinear regression analysis.

2.3. Bcl-2, Bcl-xL and Mcl-1 bind Bmf BH3 through a hydrophobic groove

Bcl-2, Bcl-xL and Mcl-1 interact with the Bmf BH3 peptide in a canonical mode. The Bmf BH3 peptide folds into an α-helix and inserts into the hydrophobic groove of Bcl-2, Bcl-xL or Mcl-1. Four hydrophobic residues of Bmf BH3, Ile-133, Leu-137, Ile-140 and Phe-144, occupy the four hydrophobic pockets of Bcl-2, Bcl-xL and Mcl-1, while the conserved Asp-142 and other polar residues of Bmf BH3 form hydrophilic interaction on either side of the grooves (Fig. 2A-C). The shapes of the small hydrophobic pockets and surface electrostatic potential of Bcl-2, Bcl-xL and Mcl-1 are different.

Bcl-2 and Bcl-xL are highly conserved pro-survival Bcl-2 family proteins, with 45 % sequence identity (Fig. S1). They both bind potently to Bmf BH3. The complex structures of Bcl-2/Bmf BH3 and Bcl-xL/Bmf BH3 provide a molecular mechanism for the high binding affinity. In the Bcl-2/Bmf structure, Ile-133^{Bmf} at h1 position interacts with Val-133^{Bcl-2} and Leu-119^{Bcl-2} in the P1 pocket (Fig. 2D). Phe-153^{Bcl-2} and Phe-112^{Bcl-2} constitute the bottom of P2 and P3 pockets, and are surrounded by residues Met-115^{Bcl-2}, Leu-137^{Bcl-2}, Ala-149^{Bcl-2}, Phe-104^{Bcl-2} and Tyr-108^{Bcl-2} to ensure hydrophobic interactions with h2 and h3 residues Leu-137^{Bmf} and Ile-140^{Bmf}. The h4 residue Phe-144^{Bmf} is stretched to the distal P4 pocket and interacts with Ala-100^{Bcl-2}, Gly-145^{Bcl-2} and Val-148^{Bcl-2}. These hydrophobic residues involved in interactions with Bmf BH3 are mostly conserved between Bcl-2 and Bcl-xL (Fig. 2E). However, the orientation flip of Tyr-101^{Bcl-xL} and Phe-105^{Bcl-xL} at the α2-α3 corner of Bcl-xL results in some obvious differences in the P3 pocket and the edges. Tyr-101^{Bcl-xL} (corresponding to Tyr-108^{Bcl-2}) constitutes the edge of P2 pocket and the base of P3 pocket of Bcl-xL, whereas Phe-105^{Bcl-xL} (corresponding to Phe-112^{Bcl-2}) is exposed to solvent.

In the Mcl-1/Bmf BH3 complex, Bmf BH3 is also accommodated in the hydrophobic groove of Mcl-1. Mcl-1 residues are conserved with those of Bcl-2 and Bcl-xL, such as P1 pocket, Phe-270^{Mcl-1} and Phe-228^{Mcl-1} in the bottom of P2 and P3 pockets (Fig. 2F). However, this conserved Phe-270^{Mcl-1} orientates α3 helix of Mcl-1, while the homologous Phe-153^{Bcl-2} (or Phe-146^{Bcl-xL}) orientates α4 helix. Distinct from Bcl-2 and Bcl-xL, the P4 pocket of Mcl-1 is much flatter and has shallower interaction with the h4 residue Phe-44^{Bmf} (Fig. 2C, F). Thr-266^{Mcl-1}, His-224^{Mcl-1}, Val-220^{Mcl-1} and Val-216^{Mcl-1} in the periphery of P3 pocket and P4 pocket are non-conserved with the corresponding residues in Bcl-2 and Bcl-xL (Fig. 2G). Overall, Bcl-2 and Bcl-xL have similar

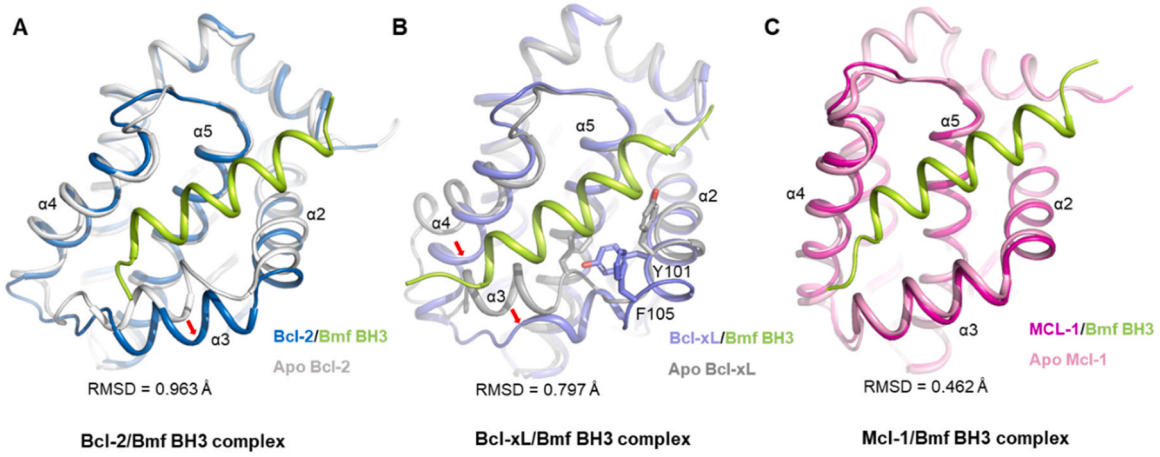

Fig. 1. The overall structures of Bmf BH3 in complex with Bcl-2, Bcl-xL and Mcl-1. A, Cartoon representation of the structural comparison of Bcl-2/Bmf BH3 with Apo Bcl-2 (PDB ID 1G5M). B, Cartoon representation of the structural comparison of Bcl-xL/Bmf BH3 with Apo Bcl-xL (PDB ID 1MAZ). The orientation of Tyr-101 and Phe-105 are shown as sticks. C, Cartoon representation of the structural comparison of Mcl-1/Bmf BH3 with Apo Mcl-1 (PDB ID 6QB3).

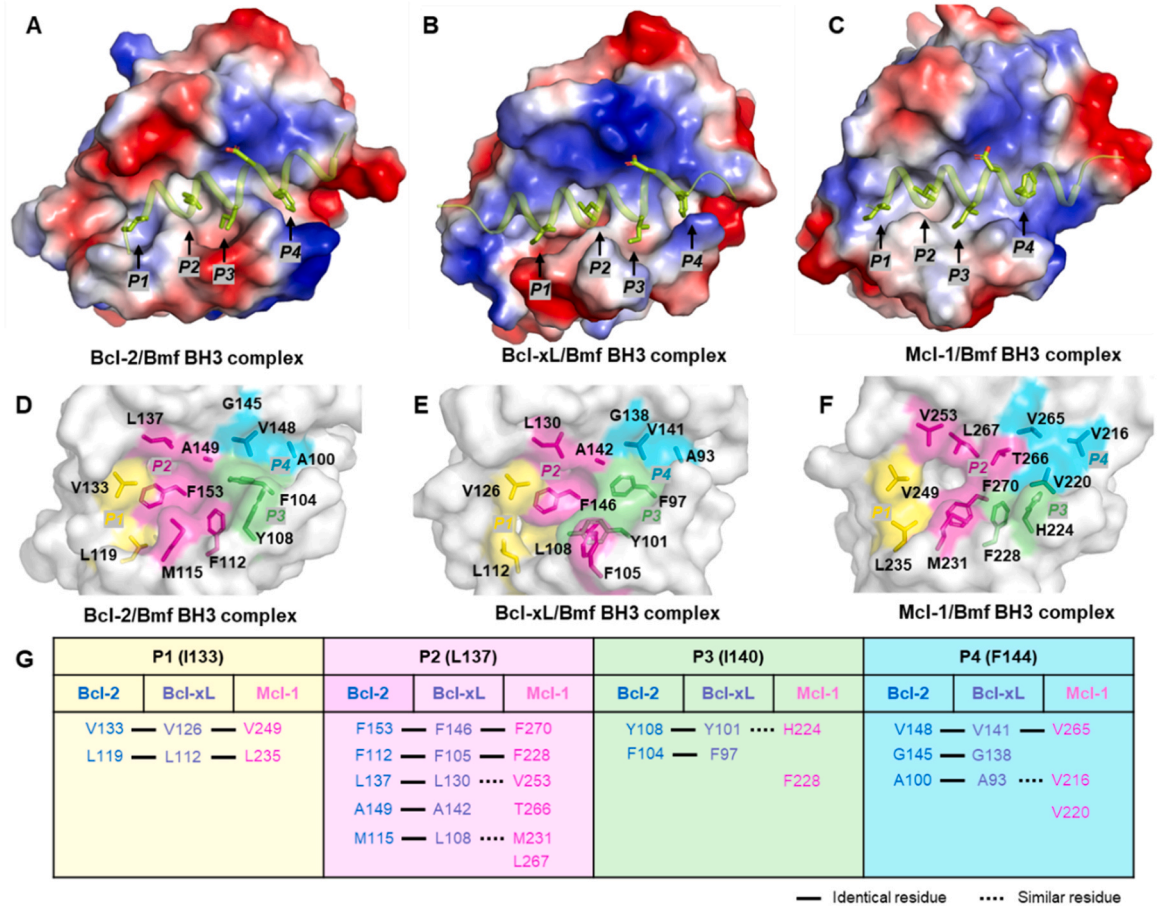

Fig. 2. Comparison of hydrophobic pockets of Bcl-2, Bcl-xL, and Mcl-1. A-C, Electrostatic potential surface view of Bcl-2, Bcl-xL and Mcl-1. The Bmf BH3 peptide is shown as cartoon. Four hydrophobic residues (h1, h2, h3, h4) and the Asp-142 are shown as sticks. D-F, Surface representation of the BH3 binding groove of Bcl-2, Bcl-xL and Mcl-1. The four hydrophobic pockets (P1-P4) and residues are highlighted and labelled. G, Hot-spots residues in P1-P4 pockets of Bcl-2, Bcl-xL and Mcl-1.

interactions with Bmf BH3, with only some differences in conformational changes, whereas Mcl-1 has distinct interactions with Bmf BH3.

2.4. Comparison of the interface of Bmf BH3 with Bcl-2, Bcl-xL and Mcl-1

In addition to the hydrophobic P1-P4 pockets, hydrophilic contacts also play critical roles in the interaction of Bcl-2, Bcl-xL and Mcl-1 with Bmf BH3. At the α4-α5 region, a highly conserved salt bridge interaction is canonically observed between the conserved Asp of BH3 domain and the conserved Arg of Bcl-2, Bcl-xL and Mcl-1. The Asp-142^{Bmf} at h3 + 2 position also formed a conserved salt bridge interaction with Arg-146^{Bcl-2} (Fig. 3A) or Arg-139^{Bcl-xL} (Fig. 3C). Other hydrophilic contacts are mainly contributed by non-conserved residues of Bmf BH3. For Bcl-2,

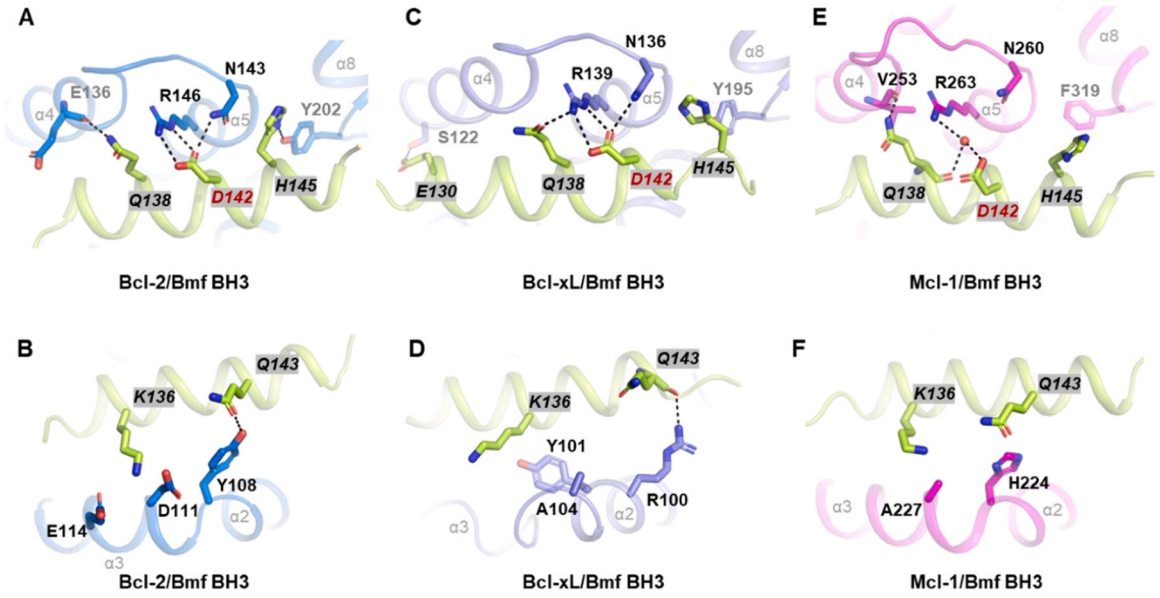

Fig. 3. Detailed contacts in the Bcl-2/Bmf BH3, Bcl-xL/Bmf BH3 and Mcl-1/Bmf BH3 complex. A-C, Detailed interactions of Bmf BH3 with the α4-α5 helix of Bcl-2, Bcl-xL and Mcl-1. D-F, Detailed interactions of Bmf BH3 with the α2-α3 helix of Bcl-2, Bcl-xL and Mcl-1. The involved residues are shown as sticks. The black lines represent hydrogen bonds. The red spheres represent water molecules.

Gln-138^{Bmf} at h2 + 1 position establishes hydrogen bond interactions with Leu-136^{Bcl-2}, as well as hydrogen bond interactions with the backbone of α4 (Fig. 3A). For Bcl-xL, Gln-138^{Bmf} at h2 + 1 position establishes hydrogen bond interactions with Arg-139^{Bcl-xL} (Fig. 3C). His-145^{Bmf} at h4 + 1 position interacts with Tyr-202^{Bcl-2} at the C-terminal α8 helix. At the α2-α3 region, side chain of Gln-143^{Bmf} at h3 + 3 position forms a direct hydrogen bond with Tyr-108^{Bcl-2}(Fig. 3B), while a hydrogen bond is formed between Gln-143^{Bmf} backbone and Arg-100^{Bcl-xL} (Fig. 3D). In addition, although the density of the basic group of Lys-136^{Bmf} at h1 + 3 position is weak, the positively charged Lys-136^{Bmf} is likely to be attracted by the negatively charged α3 of Bcl-2 (Asp-111^{Bcl-2}, Glu114^{Bcl-2}) (Fig. S2A). Notably, h1–3 position of Glu-130^{Bmf} interacts with the N-terminal α4 helix of Ser-122^{Bcl-xL}, and this hydrogen bond is also observed in the structure of Bcl-xL with Bim BH3 [31] (Fig. S3B–C), which may explain the N-terminal extension of the Bmf BH3 peptide contributing to crystallization with Bcl-xL.

Compared to Bcl-2 and Bcl-xL, Mcl-1 has little hydrophilic interaction to help stabilize Bmf BH3. First of all, the conserved Asp-142^{Bmf} did not form a salt bridge with Arg-263^{Mcl-1}, but instead formed a water-mediated hydrogen bond (Fig. 3E). Gln-138^{Bmf} at h2 + 1 position only contributes a hydrogen bond with backbone of α4 (Fig. 3E). Electrostatic and hydrogen bond interactions were not observed in the C-terminal α8 helix and α2-α3 region (Fig. 3F). Overall, deficiency of electrostatic and hydrogen-bond interactions in Mcl-1/Bmf BH3 complex may be a major reason for their lower binding affinity.

2.5. Role of Bcl-2, Bcl-xL, and Mcl-1 mutations on Bmf BH3 interactions

To better characterize the determinants for different pro-survival Bcl-2 family proteins to Bmf BH3, we mutated the conserved Arg and the involved α2-α3 residues of Bcl-2, Bcl-xL and Mcl-1, and then measured the binding affinity of these mutants to Bmf BH3 by FP assay. The Kd values of R146A^{Bcl-2}, R139A^{Bcl-xL} and R263A^{Mcl-1} to FITC-Bmf were 622.6 nM, 1.24 μM and 49 μM (Fig. 4A-C), respectively. Consistently, mutations of the conserved Arg reduced the binding affinity of Bcl-2 and Bcl-xL to Bmf BH3 by 120 and 240 folds, respectively. Unexpectedly, although Arg-263^{Mcl-1} did not form salt bridge interactions with Bmf, the mutant R263A^{Mcl-1} also caused a 260-fold reduction in

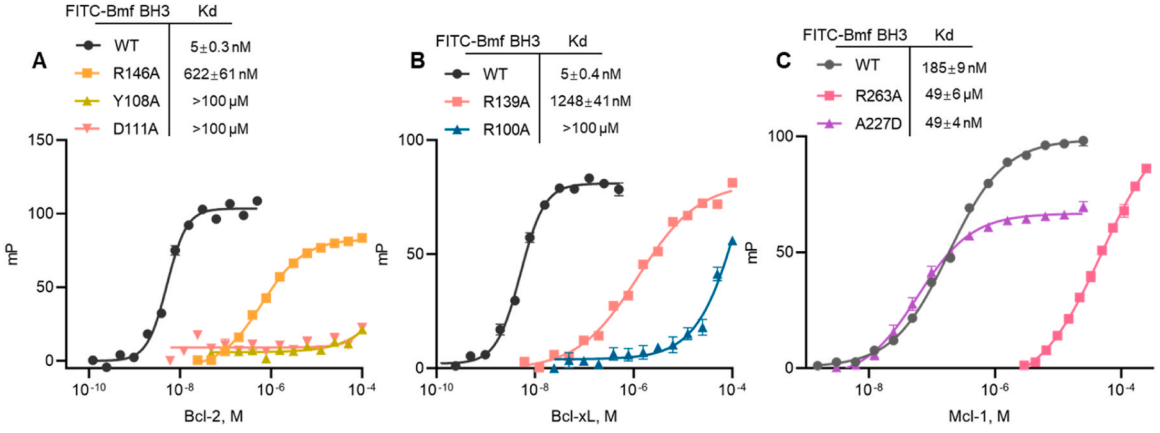

Fig. 4. Binding affinity of Bcl-2, Bcl-xL and Mcl-1 mutants to Bmf BH3. A-C, Fluorescence polarization assay was performed to determine the Kd values of fluorescently labeled Bmf BH3 bound to WT or mutant Bcl-2, Bcl-xL and Mcl-1. Kd was determined by nonlinear regression analysis. Data are represented as the mean ± SD of 3–4 independent experiments. WT, wild-type.

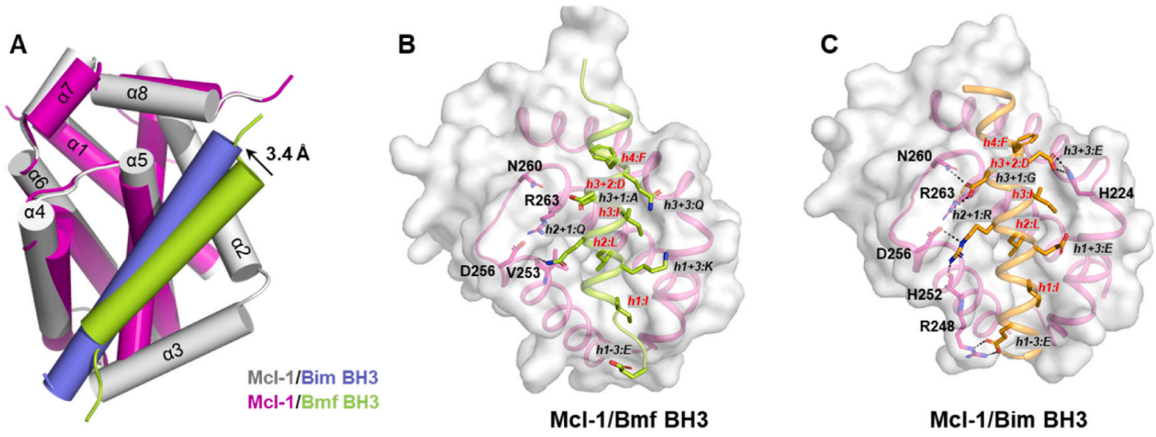

D

	h1 h2 h3 h4	Bcl-2	Bcl-xL	Mcl-1
Bim:	MRPEIWIAQELRRIGDEFNAYYARR	20±0.6 nM	33±6 nM	19±3 nM
Bmf:	HQAEVQIARKLQCIADQFHRLHVQQ	18±0.2 nM	23±0.3 nM	12±1 μM
Bmf-m1:	HQAEVQIARKLRCIADQFHRLHVQQ	18±0.6 nM	31±2 nM	6.5±0.4 μM
Bmf-m2:	HQAEVQIARKLQCIGDQFHRLHVQQ	38±1 nM	97±1 nM	1.4±0.5 μM
Bmf-m3:	HQAEVQIARKLQCIADEFHRLHVQQ	17±0.3 nM	29±0.2 nM	8.9±1 μM
Bmf-m4:	HQAEVQIARKLRCIADEFHRLHVQQ	23±1 nM	27±0.5 nM	1.7±0.2 μM
Bmf-m5:	HQAEVQIARKLRCIGDEFHRLHVQQ	16±1 nM	46±1 nM	61±1 nM

Fig. 5. Comparison of the interactions of Bim BH3 and Bmf BH3 with Mcl-1. A, Overlay structures of Mcl-1/Bim BH3 and Mcl-1/Bmf BH3 complexes. B, Mcl-1 in complex with Bmf BH3. C, Mcl-1 in complex with Bim BH3 (PDB ID 2PQK). The amino acids involved in the interactions are shown as sticks. Hydrogen bonds are shown as black dashed lines. D, Sequence alignment of the BH3 domain of Bim, Bmf and mutant Bmf, and their inhibition constant (Ki) for Bcl-2, Bcl-xL and Mcl-1. Fluorescence polarization competition assay was used to detect the Ki of unlabeled Bim BH3 or Bmf BH3 peptides in competition with fluorescently labeled Bim BH3 for Bcl-2, Bcl-xL, and Mcl-1. All assays were independently repeated three times and Ki was determined by one-site competition analysis.

binding affinity (Fig. 4C). This indicates that the water-mediated interaction of Arg-263^{Mcl-1} with Asp-142^{Bmf} is still essential for maintaining Mcl-1/Bmf binding.

Notably, mutations of α2-α3 residues in Bcl-2 and Bcl-xL had a significant effect on their affinity for Bmf BH3. The mutants Y108A^{Bcl-2}, D111A^{Bcl-2}, and R100A^{Bcl-xL} all showed an affinity greater than 100 μM (Fig. 4A-B). In contrast, substitution of Ala-227^{Mcl-1} with Asp at the corresponding site of Bcl-2 (D111^{Bcl-2}) increased the affinity of Mcl-1 for Bmf BH3 to 49 nM, approximately 4-fold higher than that of wild-type (Fig. 4C). These results suggest that these less conserved residues located in the α2-α3 region of Bcl-2, Bcl-xL and Mcl-1 contribute to their binding specificity to Bmf BH3.

2.6. Comparison of the interactions of Bim BH3 and Bmf BH3 with Bcl-2, Bcl-xL and Mcl-1

Several studies have reported that Bim and Bmf have similar localizations and functions [15,35–37]. Structurally, Bmf and Bim share highly similar BH3 domain, and the four hydrophobic residues (h1-h4) are identical. However, different from Bmf, Bim BH3 peptide (FITC-Bim BH3) could bind tightly to Bcl-2, Bcl-xL and Mcl-1 with Kd values of 6.1 nM, 4.4 nM and 5.8 nM, respectively (Table 1). When we used the unlabeled Bmf BH3 peptide to compete with FITC-Bim BH3 for these three pro-survival proteins, Bmf BH3 could easily interfere with Bim BH3/Bcl-2 complex and Bim BH3/Bcl-xL complex with Ki of 18 nM and 23 nM, respectively, whereas Bmf could hardly release Bim from the Bim/Mcl-1 complex with a Ki of 12 μM (Fig. 5D). Overall, Bmf and Bim have different selectivities for Mcl-1.

To understand the basis of this difference, we compared the Mcl-1/Bmf BH3 structure with the Mcl-1/Bim BH3 structure (PDB: 2PQK) [38]. The Mcl-1 structures have little discrepancy in the two complexes, but the position of the BH3 domain is slightly different (Fig. 5A). The C-terminus of Bmf BH3 is shifted by about 3.4 Å. Consistent with this, Bim BH3 has a canonical salt bridge interaction with the α4-α5 region, whereas Bmf BH3 does not (Fig. 5B-C). In addition, three charged Bim BH3 residues, Glu at h1–3 position, Arg at h2 + 1 position and Glu at h3 + 3 position, are involved in polar interactions with Mcl-1 (Fig. 5C). Replacing the h2 + 1 and h3 + 3 positions of Bim BH3 with the opposite charged residues reduced its affinity to Mcl-1 [38,39]. However, these positions in Bmf are not conserved with Bim, and are not involved in direct interactions with Mcl-1. A crossed Bmf-m2 peptide replaced Ala at the h3 + 1 position with Gly, had an approximately 9-fold increase in the ability to compete for Mcl-1 from Mcl-1/FITC-Bim BH3 complex (Fig. 5D). Another Bmf-m4 peptide with h2 + 1 and h3 + 3 positions substituted with side chains of Bim, had an approximately 7-fold increase in this ability (Fig. 5D). Notably, when the h2 + 1, h3 + 3 and h3 + 1 positions of the Bmf BH3 peptide were all replaced by the Bim side chain, the resulting Bmf-m5 peptide had a Ki of 61 nM for Mcl-1 in the competitive binding assay, and the affinity was approximately 200-fold higher than that of wild-type Bmf BH3. Therefore, these non-conserved residues between Bim and Bmf contribute to their different affinities for Mcl-1.

3. Discussion

The regulation of the mitochondrial apoptotic pathway depends on the interaction of pro-survival Bcl-2 family proteins with BH3-only proteins. The BH3 domain of certain BH3-only proteins (Bim, Bid, Puma) binds all pro-survival Bcl-2 family proteins with approximate high affinity [40,41], whereas Bmf BH3 has definite specificity and binds only some of the pro-survival Bcl-2 family proteins with high affinity. These specificities may be related to the regulation of

mitochondria-dependent apoptosis by the Bcl-2 family in response to different stress stimuli [27]. Here we report structural information on Bmf BH3, a peptide derived from the BH3 domain of Bmf, in complex with Bcl-2, Bcl-xL, and Mcl-1 to help unravel the molecular basis of specific binding.

Bcl-2 and Bcl-xL share high sequence similarity, and the residues defining the hydrophobic groove are highly conserved (Fig. S1). Thus, they have a more similar spectrum for binding pro-apoptotic proteins [25,34]. In general, for all pro-survival Bcl-2 family proteins, the P2 pocket is the most important which binds an invariant Leu at h2 position of BH3. The interactions of Bcl-xL and Bcl-2 with BH3 also depend on the deep hydrophobic pocket P4 [42,43]. Consistently, most small molecule drugs, such as ABT-737 [43], ABT-263 [44,45], and ABT-199 [46] (Fig. S3), use hydrophobic groups to occupy the P2 and P4 pockets of Bcl-xL and Bcl-2 to obtain tight binding. In the Bcl-2/Bmf BH3 and Bcl-xL/Bmf BH3 complexes, the highly conserved Leu (h2) and Phe (h4) penetrate deeply into the P2 and P4 pockets. Furthermore, numerous hydrogen bond interactions help stabilize their interactions, and mutations of these hydrophilic residues in Bcl-2 and Bcl-xL greatly reduced their affinity for Bmf BH3 (Fig. 4A-B). Similar interaction patterns were also present in Bcl-xL/Bim BH3 complex (Fig. S3C) [31]. However, Bmf BH3 and Bim BH3 have different sequence at these non-conserved positions, such as h1 + 3, h2 + 1, and h3 + 3. Substitution of these non-conserved hydrophilic residues in Bmf BH3 with Bim BH3 had small effects on the affinity for Bcl-2 and Bcl-xL (Fig. 5D). Thus, hydrophilic contacts with these non-conserved residues of Bmf BH3 provide assistance for the high-affinity binding, but Bcl-2 and Bcl-xL have a low selectivity for these residues.

Mcl-1 shares only 29 % sequence identities with Bcl-2 and Bcl-xL in the Bcl-2 core domains (Fig. S1). The hydrophobic groove of Mcl-1 differs from that of Bcl-xL and Bcl-2. The P2 pocket of Mcl-1 is most important for binding, as it flexibly adapts to shape and can open to merge with P3 [47]. Except for h2 and h3, Mcl-1 is tolerant to mutations in h1 and h4 [25,38,43]. Especially, substitution of h4 in Bim does not affect its binding to Mcl-1 [43]. On the other hand, it seems that Mcl-1 is more dependent on some non-conserved residues in the BH3 domain. In the Mcl-1/Bim BH3 complex, in addition to the conserved Arg-Asp, charged residues at the h2 + 1 and h3 + 3 positions of Bim BH3 are involved in the hydrogen bonds interaction with Mcl-1 [38] (Fig. 5B). In particular, Arg at h2 + 1 forms a hydrogen bond with His-252^{Mcl-1}, which is also observed in the Mcl-1/Puma BH3 and Mcl-1/Noxa BH3 complexes [45,48] (Fig. S4). However, these hydrophilic interactions are absent in the Mcl-1/Bmf complex. Substitution of the h2 + 1 and h3 + 3 positions of Bmf BH3 with residues of Bim enhances the affinity for Mcl-1.

In addition, Mcl-1 prefers a smaller amino acid at h3 + 1 position. The position in Bim BH3 is a Gly, while Bmf BH3 is an Ala. The h3 + 1 position in the BH3 sequence is usually occupied by small amino acids, particularly in Mcl-1/Bim BH3 interaction, which does not accommodate substitutions of residues larger than Gly [42,49]. For Bmf BH3, the side chain of Ala-141 is close to Mcl-1 residues Gly-262, Thr-266 and the conserved Arg-146 (Fig. 5B-C), which may increase the spatial distance to the interaction of Asp-142^{Bmf} at h3 + 2 with the conserved Arg146^{Mcl-1}. In agreement with this, a crossed Bmf BH3 peptide with h3 + 1 position substituted with Gly, resulted in an approximately 9-fold increase in the ability to compete for Mcl-1 from Mcl-1/FITC-Bim BH3 complex (Fig. 5D). The h3 + 1 position of Bad BH3 is a larger amino acid Ser, and Bad BH3 has been shown to have low binding affinity for Mcl-1 (>1 μM) [50]. Our data indicate that the h2 + 1, h3 + 3, and h3 + 1 positions of Bmf BH3 with Bim residues increased its affinity for Mcl-1 by about 200-fold (Fig. 5D). Overall, these non-conserved residues in BH3 domain of Bmf have an important role for its affinity to pro-survival Bcl-2 family proteins.

Although the structure of the full-length BH3-only protein has not been determined, it has been shown that short peptides from the BH3 domain of BH3-only proteins could bind to pro-survival Bcl-2 proteins and promote apoptosis [51,52]. However, it is noted that in our experiments, truncated proteins and short peptides were used to facilitate protein purification and crystallization. They may not fully represent intact proteins and may differ to some extent in conformation from full-length proteins in the cellular context. A substantial challenge for the future is to express full-length BH3-only proteins and observe their interaction with intact pro-survival Bcl-2 family proteins.

In summary, the interaction affinity between the Bmf BH3 domain and the pro-survival Bcl-2 proteins varies more than 35-fold. Our structural determination of the Bmf BH3 in complex with truncated Bcl-2, Bcl-xL, and Mcl-1 elucidates the molecular basis for this specific binding. The overall topology of the complex shows that the Bmf BH3 peptide occupies the hydrophobic pocket of Bcl-2, Bcl-xL, and Mcl-1 with four hydrophobic residues. Nevertheless, the differences in the BH3 sequence and the groove of pro-survival Bcl-2 family proteins result in different specificities and selectivities. Our detailed structural and mutation analyses provide new insights into the development of selective BH3 mimetic drugs targeting pro-survival Bcl-2 family proteins.

4. Materials and methods

4.1. Plasmids

Recombinant human Bcl-2ΔC32 and Bcl-xLΔC25 was cloned into vector pET28a (Novagen, 69864-3). Recombinant human Mcl-1 (ΔN170ΔC23) was cloned into a modified pET28a vector with a N-terminal His-SUMO tag. The human Bcl-2 construct used for crystallization (Bcl-2ΔC32ΔLoop) replaces the unstructured loop between residues 35–92 with residues 29–44 of Bcl-xL. The human Bcl-xL construct for crystallization (Bcl-xLΔC25ΔLoop) removes the unstructured loop between residues 46–82. All plasmids were performed according to the manufacturer's instructions for the ClonExpress II One Step Cloning Kit (Vazyme, C112). All mutants were constructed by PCR mutagenesis using the KOD Plus mutagenesis kit (TOYOBO, SMK-101) using the wild-type plasmid as the template.

4.2. Protein expression and purification

Plasmids were transfected into in Escherichia coli Rosetta BL21 (DE3) cells. The cells were cultured at 37 °C in LB culture medium and then induced by 0.5 mM isopropyl β-D-1-thiogalactoside (IPTG) at 18 °C for 12 h. The fused His-SUMO-Mcl-1, His-Bcl-2 and His-Bcl-xL proteins were purified by nickel affinity chromatography. The N-terminal His-SUMO tag or His tag were removed by ULP1 protease or PreScission protease at 4 °C. Untagged protein was purified by size exclusion chromatography (Superdex 200 10/300 GL, GE Healthcare, 17–5175–01) with 20 mM Tris, pH 8.0, 150 mM NaCl, and 0.5 mM TCEP. Peak fractions were collected and concentrated to 10 mg/ml, and stored at −80 °C until use.

4.3. Peptides

All peptides were synthesized and purchased from GenScript. Fluorescent peptide sequences were as follows: FITC-Bim, RPEIWIAQELRRIGD(K-FITC)FNAYYA; FITC-Bmf, FITC-HQAEVQIARKLQCIADQFHRLHVQQ. Peptide sequences were as follows: 25-mer Bmf, HQAEVQIARKLQCIADQFHRLHVQQ, for crystallization with Bcl-xL; 21-mer Bmf, EVQIARKLQCIADQFHRLHVQ, for crystallization with Mcl-1 and Bcl-2.

4.4. Crystallization and structure determination

For crystallization, Bcl-2, Bcl-xL and Mcl-1 were mixed with excess BH3 domain peptide in a 1:1.5 molar ratio. Crystals were grown at 18 °C by hanging drop vapor diffusion from drops containing 1 μl protein and 1 μl reservoir solution. Crystals of Bmf BH3 complexed with Bcl-2 were

grown in a reservoir buffer containing 0.1 M potassium thiocyanate and 25 % polyethylene glycol monomethyl ether % 2000. Crystals of Bmf BH3 complexed with Bcl-xL were grown in a reservoir buffer containing 0.2 M sodium chloride, 0.1 M sodium acetate: acetic acid, pH 4.5 and 1.26 M ammonium sulfate. Crystals of Bmf BH3 complexed with Mcl-1 were grown in a reservoir buffer containing 0.1 M potassium thiocyanate and 20 % polyethylene glycol monomethyl ether 2000.

For data collection, a single crystal was equilibrated in cryoprotectant consisting of reservoir solution supplemented with 20 % (v/v) ethylene glycol and then flash-frozen in liquid nitrogen. Data were collected at beamline BL02U of the Shanghai Synchrotron Radiation Facility (SSRF). HKL3000 was used to processes the data [53]. Structures were determined by molecular replacement using Phenix.phaser [54]. The structure, Mcl-1 (PDB: 6O6F) Bcl-2 (PDB: 2XA0) and Bcl-xL (PDB: 4QVF) were used as search templates. The initial model was manually built by the program Coot and refinement was performed with Phenix.refine [55,56]. Translational-liberation-screw (TLS) refinement was used during the last stages of refinement. Graphical representations of the structure were generated using PyMOL [57].

4.5. Fluorescence polarization assay (FP)

Binding assays were performed as previously described [58]. Proteins were serially diluted in buffer (20 mM Tris pH 8.0, 50 mM NaCl) and subsequently injected into 384-well black Corning plates (Corning #4815) along with FITC BH3 (10 nM). Multiwell plates were mixed on a shaker for 1 min and then incubated for another 10 min at room temperature in the dark. Polarization in milli-polarization units (mP) was measured with a microplate reader (PerkinElmer Envision). At least three replicates of each experiment were performed. All experimental data were analyzed for dissociation constants (Kd) by sigmoidal dose-response nonlinear regression model of GraphPad Prism software [58,59].

4.6. Fluorescence polarization competition assay (FPA)

Binding assays were performed as previously described [58]. For the peptide inhibition studies, serial dilutions of BH3 peptide were mixed with FITC BH3 (10 nM) and then proteins diluted in binding buffer was added. 384 plates were mixed on a shaker for 1 min and then incubated in the dark at room temperature until equilibrium is reached. At least three replicates of each experiment were performed. Polarization in milli-polarization units (mP) was measured with a microplate reader (PerkinElmer Envision). All experimental data were analyzed for inhibition constant (Ki) by one-site competition model of GraphPad Prism software [58,60].

4.7. Accession numbers

The atomic coordinate and structure factor for Bcl-2/Bmf, Bcl-xL/Bmf, Mcl-1/Bmf complexes have been deposited with the Protein Data bank under accession code 8IQL, 8IQK and 8IQM.

CRediT authorship contribution statement

Haolan Wang: Conceptualization, Investigation, Writing - original draft. **Ming Guo:** Review & editing. **Hudie Wei:** Writing - review & editing. **Yongheng Chen:** Review & editing, Supervision.

Declaration of Competing Interest

The authors declare that they have no known competing financial interests or personal relationships that could have appeared to influence the work reported in this paper.

Acknowledgments

We thank the staff from the Shanghai Synchrotron Radiation facility (SSRF) beamline BL02U1 for assistance during diffraction data collection. This work was financially supported by the Natural Science Foundation of China (No. 81570537, 81974074, 82172654, 82273496 and 31900880), Hunan Provincial Science and Technology Department (2018RS3026 and 2021RC4012), Natural Science Foundation of Hunan Province (2023JJ20092 and 2023JJ30863), and Central South University Innovation-Driven Research Programme (2023CXQD076).

Appendix A. Supporting information

Supplementary data associated with this article can be found in the online version at doi:10.1016/j.csbj.2023.07.017.

References

[1] Delbridge A, Grabow S, Strasser A, Vaux D. Thirty years of BCL-2: translating cell death discoveries into novel cancer therapies. Nat Rev Cancer 2016;16:99–109.
[2] Singh R, Letai A, Sarosiek K. Regulation of apoptosis in health and disease: the balancing act of BCL-2 family proteins. Nat Rev Mol Cell Biol 2019;20:175–93.
[3] Czabotar PE, Westphal D, Dewson G, Ma S, Hockings C, Fairlie WD, et al. Bax crystal structures reveal how BH3 domains activate Bax and nucleate its oligomerization to induce apoptosis. Cell 2013;152:519–31.
[4] Flores-Romero H, Ros U, Garcia-Saez AJ. Pore formation in regulated cell death. EMBO J 2020;39:e105753.
[5] Moldoveanu T, Follis AV, Kriwacki RW, Green DR. Many players in BCL-2 family affairs. Trends Biochem Sci 2014;39:101–11.
[6] Wang H, Guo M, Wei H, Chen Y. Targeting MCL-1 in cancer: current status and perspectives. J Hematol Oncol 2021;14:67.
[7] Dewson G, Kratina T, Sim HW, Puthalakath H, Adams JM, Colman PM, et al. To trigger apoptosis, Bak exposes its BH3 domain and homodimerizes via BH3:groove interactions. Mol Cell 2008;30:369–80.
[8] Suzuki M, Youle RJ, Tjandra N. Structure of Bax: coregulation of dimer formation and intracellular localization. Cell 2000;103:645–54.
[9] O'Neill KL, Huang K, Zhang J, Chen Y, Luo X. Inactivation of prosurvival Bcl-2 proteins activates Bax/Bak through the outer mitochondrial membrane. Genes Dev 2016;30:973–88.
[10] Huang K, O'Neill KL, Li J, Zhou W, Han N, Pang X, et al. BH3-only proteins target BCL-xL/MCL-1, not BAX/BAK, to initiate apoptosis. Cell Res 2019;29:942–52.
[11] Wilfling F, Weber A, Potthoff S, Vögtle F, Meisinger C, Paschen S, et al. BH3-only proteins are tail-anchored in the outer mitochondrial membrane and can initiate the activation of Bax. Cell Death Differ 2012;19:1328–36.
[12] Montero J, Haq R. Adapted to survive: targeting cancer cells with BH3 mimetics. Cancer Discov 2022;12:1217–32.
[13] Diepstraten ST, Anderson MA, Czabotar PE, Lessene G, Strasser A, Kelly GL. The manipulation of apoptosis for cancer therapy using BH3-mimetic drugs. Nat Rev Cancer 2022;22:45–64.
[14] Puthalakath H, Villunger A, O'Reilly LA, Beaumont JG, Coultas L, Cheney RE, et al. Bmf: a proapoptotic BH3-only protein regulated by interaction with the myosin V actin motor complex, activated by anoikis. Science 2001;293:1829–32.
[15] Singh PK, Roukounakis A, Weber A, Das KK, Sohm B, Villunger A, et al. Dynein light chain binding determines complex formation and posttranslational stability of the Bcl-2 family members Bmf and Bim. Cell Death Differ 2020;27:434–50.
[16] Hunt A, Evan G. Apoptosis. Till death us do part. Science 2001;293:1784–5.
[17] Piñon JD, Labi V, Egle A, Villunger A. Bim and Bmf in tissue homeostasis and malignant disease. Oncogene 2008;27(Suppl 1):S41–52.
[18] Woess C, Tuzlak S, Labi V, Drach M, Bertele D, Schneider P, et al. Combined loss of the BH3-only proteins Bim and Bmf restores B-cell development and function in TACI-Ig transgenic mice. Cell Death Differ 2015;22:1477–88.
[19] Labi V, Woess C, Tuzlak S, Erlacher M, Bouillet P, Strasser A, et al. Deregulated cell death and lymphocyte homeostasis cause premature lethality in mice lacking the BH3-only proteins Bim and Bmf. Blood 2014;123:2652–62.
[20] Kutuk O, Letai A. Displacement of Bim by Bmf and Puma rather than increase in Bim level mediates paclitaxel-induced apoptosis in breast cancer cells. Cell Death Differ 2010;17:1624–35.
[21] Brouwer JM, Lan P, Cowan AD, Bernardini JP, Birkinshaw RW, van Delft MF, et al. Conversion of Bim BH3 from activator to inhibitor of bak through structure-based design. Mol Cell 2017;68.
[22] Robin AY, Krishna Kumar K, Westphal D, Wardak AZ, Thompson GV, Dewson G, et al. Crystal structure of Bax bound to the BH3 peptide of Bim identifies important contacts for interaction. Cell Death Dis 2015;6:e1809.
[23] Du H, Wolf J, Schafer B, Moldoveanu T, Chipuk JE, Kuwana T. BH3 domains other than Bim and Bid can directly activate Bax/Bak. J Biol Chem 2011;286:491–501.
[24] Ye K, Meng WX, Sun H, Wu B, Chen M, Pang Y-P, et al. Characterization of an alternative BAK-binding site for BH3 peptides. Nat Commun 2020;11:3301.
[25] Chen L, Willis SN, Wei A, Smith BJ, Fletcher JI, Hinds MG, et al. Differential targeting of prosurvival Bcl-2 proteins by their BH3-only ligands allows complementary apoptotic function. Mol Cell 2005;17:393–403.

[26] Jagani H, Kasinathan N, Meka SR, Josyula VR. Antiapoptotic Bcl-2 protein as a potential target for cancer therapy: a mini review. Artif Cells Nanomed Biotechnol 2016;44:1212–21.
[27] Kim H, Rafiuddin-Shah M, Tu H-C, Jeffers JR, Zambetti GP, Hsieh JJD, et al. Hierarchical regulation of mitochondrion-dependent apoptosis by BCL-2 subfamilies. Nat Cell Biol 2006;8:1348–58.
[28] Petros AM, Medek A, Nettesheim DG, Kim DH, Yoon HS, Swift K, et al. Solution structure of the antiapoptotic protein bcl-2. Proc Natl Acad Sci U S A 2001;98:3012–7.
[29] Muchmore SW, Sattler M, Liang H, Meadows RP, Harlan JE, Yoon HS, et al. X-ray and NMR structure of human Bcl-xL, an inhibitor of programmed cell death. Nature 1996;381:335–41.
[30] Luptak J, Bista M, Fisher D, Flavell L, Gao N, Wickson K, et al. Antibody fragments structurally enable a drug-discovery campaign on the cancer target Mcl-1. Acta Crystallogr D Struct Biol 2019;75:1003–14.
[31] Rajan S, Choi M, Baek K, Yoon HS. Bh3 induced conformational changes in Bcl-Xl revealed by crystal structure and comparative analysis. Proteins 2015;83:1262–72.
[32] Sattler M, Liang H, Nettesheim D, Meadows RP, Harlan JE, Eberstadt M, et al. Structure of Bcl-xL-Bak peptide complex: recognition between regulators of apoptosis. Science 1997;275:983–6.
[33] Follis AV, Chipuk JE, Fisher JC, Yun M-K, Grace CR, Nourse A, et al. PUMA binding induces partial unfolding within BCL-xL to disrupt p53 binding and promote apoptosis. Nat Chem Biol 2013;9:163–8.
[34] Ku B, Liang C, Jung JU, Oh B-H. Evidence that inhibition of BAX activation by BCL-2 involves its tight and preferential interaction with the BH3 domain of BAX. Cell Res 2011;21:627–41.
[35] Fan J, Zhang Q, Tochio H, Li M, Zhang M. Structural basis of diverse sequence-dependent target recognition by the 8 kDa dynein light chain. J Mol Biol 2001:**306**.
[36] Zhi Z, Ouyang Z, Ren Y, Cheng Y, Liu P, Wen Y, et al. Non-canonical phosphorylation of Bmf by p38 MAPK promotes its apoptotic activity in anoikis. Cell Death Differ 2022;29:323–36.
[37] Akhter R, Saleem S, Saha A, Biswas SC. The pro-apoptotic protein Bmf co-operates with Bim and Puma in neuron death induced by β-amyloid or NGF deprivation. Mol Cell Neurosci 2018;88:249–57.
[38] Fire E, Gullá SV, Grant RA, Keating AE. Mcl-1-Bim complexes accommodate surprising point mutations via minor structural changes. Protein Sci 2010;19:507–19.
[39] Boersma MD, Sadowsky JD, Tomita YA, Gellman SH. Hydrophile scanning as a complement to alanine scanning for exploring and manipulating protein-protein recognition: application to the Bim BH3 domain. Protein Sci 2008;17:1232–40.
[40] Villalobos-Ortiz M, Ryan J, Mashaka TN, Opferman JT, Letai A. BH3 profiling discriminates on-target small molecule BH3 mimetics from putative mimetics. Cell Death Differ 2020:**27**.
[41] Herbaux C, Kornauth C, Poulain S, Chong SJF, Collins MC, Valentin R, et al. BH3 profiling identifies ruxolitinib as a promising partner for venetoclax to treat T-cell prolymphocytic leukemia. Blood 2021;137:3495–506.
[42] Dutta S, Gullá S, Chen TS, Fire E, Grant RA, Keating AE. Determinants of BH3 binding specificity for Mcl-1 versus Bcl-xL. J Mol Biol 2010;398:747–62.
[43] Lee EF, Czabotar PE, Smith BJ, Deshayes K, Zobel K, Colman PM, et al. Crystal structure of ABT-737 complexed with Bcl-xL: implications for selectivity of antagonists of the Bcl-2 family. Cell Death Differ 2007;14:1711–3.
[44] Souers AJ, Leverson JD, Boghaert ER, Ackler SL, Catron ND, Chen J, et al. ABT-199, a potent and selective BCL-2 inhibitor, achieves antitumor activity while sparing platelets. Nat Med 2013;19:202–8.
[45] Murray JB, Davidson J, Chen I, Davis B, Dokurno P, Graham CJ, et al. Establishing drug discovery and identification of hit series for the anti-apoptotic proteins, Bcl-2 and Mcl-1. ACS Omega 2019;4:8892–906.
[46] Birkinshaw RW, Gong J-N, Luo CS, Lio D, White CA, Anderson MA, et al. Structures of BCL-2 in complex with venetoclax reveal the molecular basis of resistance mutations. Nat Commun 2019;10:2385.
[47] Denis C, Sopková-de Oliveira Santos J, Bureau R, Voisin-Chiret AS. Hot-Spots of Mcl-1 protein. J Med Chem 2020;63:928–43.
[48] Czabotar PE, Lee EF, van Delft MF, Day CL, Smith BJ, Huang DCS, et al. Structural insights into the degradation of Mcl-1 induced by BH3 domains. Proc Natl Acad Sci U S A 2007;104:6217–22.
[49] Lee EF, Fairlie WD. The Structural Biology of Bcl-x. Int J Mol Sci 2019:**20**.
[50] Fenton RG, Cramer ML, Thompson RB, Zhang B. Affinities of Mcl-1 and Bcl-XL for BH3-only proteins define distinct survival functions at the outer mitochondrial membrane of multiple myeloma cells. Blood 2004;104:788-.
[51] Letai A, Bassik MC, Walensky LD, Sorcinelli MD, Weiler S, Korsmeyer SJ. Distinct BH3 domains either sensitize or activate mitochondrial apoptosis, serving as prototype cancer therapeutics. Cancer Cell 2002;2:183–92.
[52] Kuwana T, Bouchier-Hayes L, Chipuk JE, Bonzon C, Sullivan BA, Green DR, et al. BH3 domains of BH3-only proteins differentially regulate Bax-mediated mitochondrial membrane permeabilization both directly and indirectly. Mol Cell 2005;17:525–35.
[53] Minor W, Cymborowski M, Otwinowski Z, Chruszcz M. HKL-3000: the integration of data reduction and structure solution–from diffraction images to an initial model in minutes. Acta Crystallogr Sect D Biol Crystallogr 2006;62:859–66.
[54] McCoy AJ, Grosse-Kunstleve RW, Adams PD, Winn MD, Storoni LC, Read RJ. Phaser crystallographic software. J Appl Crystallogr 2007;40:658–74.
[55] Afonine PV, Grosse-Kunstleve RW, Echols N, Headd JJ, Moriarty NW, Mustyakimov M, et al. Towards automated crystallographic structure refinement with phenix.refine. Acta Crystallogr Sect D Biol Crystallogr 2012;68:352–67.
[56] Emsley P, Cowtan K. Coot: model-building tools for molecular graphics. Acta Crystallogr Sect D Biol Crystallogr 2004;60:2126–32.
[57] Warren LD. PyMOL User's Guide. San Carlos: Delano Scientific; 2004.
[58] Zhang H, Nimmer P, Rosenberg SH, Ng S-C, Joseph M. Development of a high-throughput fluorescence polarization assay for Bcl-x(L). Anal Biochem 2002;307:70–5.
[59] Pitter K, Bernal F, Labelle J, Walensky LD. Dissection of the BCL-2 family signaling network with stabilized alpha-helices of BCL-2 domains. Methods Enzym 2008;446:387–408.
[60] Stewart ML, Fire E, Keating AE, Walensky LD. The MCL-1 BH3 helix is an exclusive MCL-1 inhibitor and apoptosis sensitizer. Nat Chem Biol 2010;6:595–601.